

ENCLOSURE 4

Westinghouse Non-Proprietary

WCAP-16650-NP, Rev. 0

“Analysis of the Probability of the Generation of Missiles from Fully Integral Nuclear Low Pressure
Turbines”

(Non-Proprietary)

Westinghouse Non-Proprietary Class 3

WCAP-16650-NP
Revision 0

February 2007

Analysis of the Probability of the Generation of Missiles from Fully Integral Nuclear Low Pressure Turbines



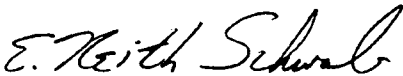
WESTINGHOUSE NON-PROPRIETARY CLASS 3

WCAP-16650-NP
Revision 0

Analysis of the Probability of the Generation of Missiles for AP1000 Fully Integral Low Pressure Turbines

Toshiba Corporation

February 2007

Reviewer: 
E. K. Schwab, Sr. Engineer
AP1000 Projects


Approved: 
M. M. Corletti, Manager
AP1000 BOP Engineering

TABLE OF CONTENTS

LIST OF TABLES	4
LIST OF FIGURES	5
1. ABSTRACT	6
2. INTRODUCTION	7
3. DESIGN FEATURES	8
3.1 MATERIAL FEATURES	9
4. PROBABILITY OF MISSILE GENERATION	10
4.1 DUCTILE BURST FROM DESTRUCTIVE OVERSPEED	10
4.2 FRACTURE RESULTING FROM HIGH CYCLE FATIGUE CRACKING	12
4.3 FRACTURE RESULTING FROM LOW-CYCLE FATIGUE - STARTUP/ SHUTDOWN CYCLES	15
4.4 FAILURE DUE TO STRESS CORROSION CRACKING	17
4.4.1 Probability of Crack Initiation	17
4.4.2 Crack Growth Rates	18
4.4.3 Critical Crack Size	20
4.4.4 Numerical Results	21
5. DISCUSSION AND CONCLUSIONS	23
6. REFERENCES	24

LIST OF TABLES

Table 4-1	Fully Integral Rotor Safety Factors Considering Ductile Bursting	6
Table 4-2	High Cycle Fatigue Peak Alternating Stresses and Safety Factors.....	9
Table 4-3	Rotor Brittle Rupture Probability Due to Startup/Shutdown Cycle Fatigue Crack Growth	11
Table 4-4	3 1/2% Ni-Cr-Mo-V Rotor Steel Deviation Crack Growth Rate from Calculation ..	14
Table 4-5	Probability of Rotor Rupture Due to Stress Corrosion	17

LIST OF FIGURES

Figure 3-1 Typical Fully Integral Rotor Construction.....	3
Figure 3-2 Typical Fully Integral Rotor Test Locations.....	4
Figure 4-1 Probability of Rotor Rupture Due to Stress Corrosion	17

1. ABSTRACT

The purpose of this report is to analyze the probability of the generation of missiles from fully integral nuclear low pressure rotors.

The potential for rotor bursting is analyzed for AP1000 low pressure turbine rotors. Four failure mechanisms are evaluated: destructive overspeed, high cycle fatigue, low cycle fatigue, and stress corrosion.

Stress corrosion is found to be the dominant mechanism for determining the potential for missile generation. The probability of a rotor burst by this mechanism does not exceed $1.0\text{E-}05$ per year even after []^{b,c} years of running time based on a conservative analysis. Therefore, it is concluded that periodic in-service, safety related inspections are not required for fully integral nuclear low pressure rotors to meet NRC safety guidelines.

2. INTRODUCTION

A typical steam turbine for modern nuclear power stations consists of a double-flow high pressure element and two or three double-flow low pressure elements in tandem. The rotor of the high pressure element generally consists of a single monoblock forging with blades attached in a fashion dependent upon the specific manufacturer's preference. Until recently, the large size of nuclear low pressure rotors has necessitated that they be constructed by building together a number of individual disc forgings. One typical construction method utilizes individual discs that are shrunk on and keyed to a central shaft.

Advances in the steel making industry have extended the capability to produce large ingots and forgings, and have removed the size restrictions on low pressure rotor designs. Turbine designers recognize the advantages of this new technology, and fully integral nuclear LP rotors are now designed and manufactured. Fully integral rotors are applied to LP rotors for AP1000.

The purpose of this report is to assess the integrity and safety of the AP1000 fully integral LP rotor designs to establish requirements on the nature and frequency of in-service, safety related rotor inspections. This assessment is accomplished by evaluating the possibility of a rotor fracture, which leads to bursting and the generation of missiles. Where possible, the probability of a rotor burst is determined directly.

3. DESIGN FEATURES

A typical fully integral rotor construction is shown in Figure 3-1. A major advantage of this design compared with built-up rotors is the elimination of the disc bores and keyways. Rotors with shrunk-on discs have peak stresses at locations where the discs are keyed to the shaft. The elimination of these regions has transferred the location of peak stress from the keyways to the lower stressed blade fastening regions. To further reduce peak stresses, the blade grooves in fully integral rotors are machined with []^{b,c}. These grooves have reduced the rotor peak stresses significantly. Since the regions of peak stress are the locations where cracks are likely to initiate, this large reduction in peak stresses leads to significant reductions in the probability of a rotor burst.

An additional, and equally important, benefit derived from the peak stress reductions achieved in fully integral rotors is that lower stress levels permit the use of lower strength materials while maintaining traditional factors of safety. The fully integral rotor designs utilize forgings heat treated to minimum yield strengths of []^{b,c}, depending upon the requirements of the particular application. Many years of experience and testing of the 3 1/2% Ni-Cr-Mo-V alloy steel rotor material have demonstrated that the ductility, toughness, and resistance to stress corrosion cracking increase as the yield strength is decreased. These benefits give additional reductions of the probability of rotor fracture.

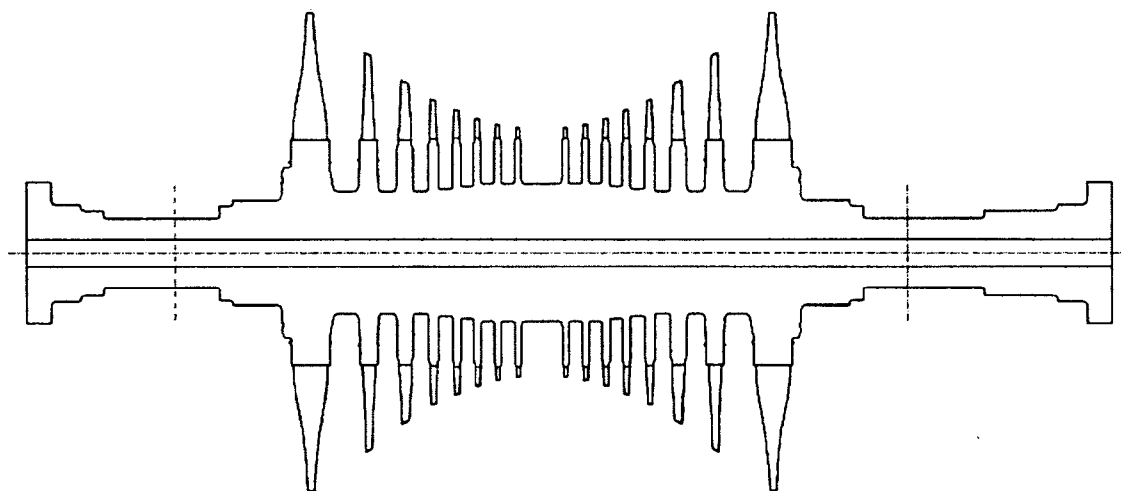


Figure 3-1 Typical Fully Integral Rotor Construction

3.1 MATERIAL FEATURES

In addition to the increased capability to manufacture very large rotor forgings, improvements in steel making practices have resulted in products with improved toughness, uniformity of properties and reductions in undesirable embrittling elements. Specifications written for fully integral rotors incorporate these enhancements.

To confirm uniformity, the specifications for fully integral nuclear rotors require testing at the locations shown in Figure 3-2. Using these specimens, tensile test, impact test, and K_{IC} measurements are performed and are used to confirm conformity to specification requirements.

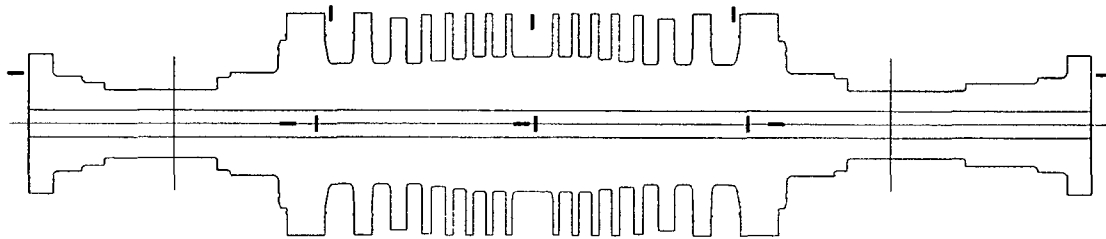


Figure 3-2 Typical Fully Integral Rotor Test Locations

4. PROBABILITY OF MISSILE GENERATION

To assess the probability of missile generation resulting from the bursting of a fully integral nuclear low pressure rotor, four potential failure mechanisms are considered:

1. Ductile burst from destructive overspeed.
2. Fracture resulting from high-cycle fatigue cracking.
3. Fracture resulting from low-cycle fatigue cracking.
4. Fracture resulting from stress corrosion cracking.

For purposes of this report, a rotor burst is considered sufficient to create a missile although it is recognized that the turbine casing offers resistance to the creation of external missiles. The methodology and results for each of the failure mechanisms analyzed are discussed in the following sections.

4.1 DUCTILE BURST FROM DESTRUCTIVE OVERSPEED

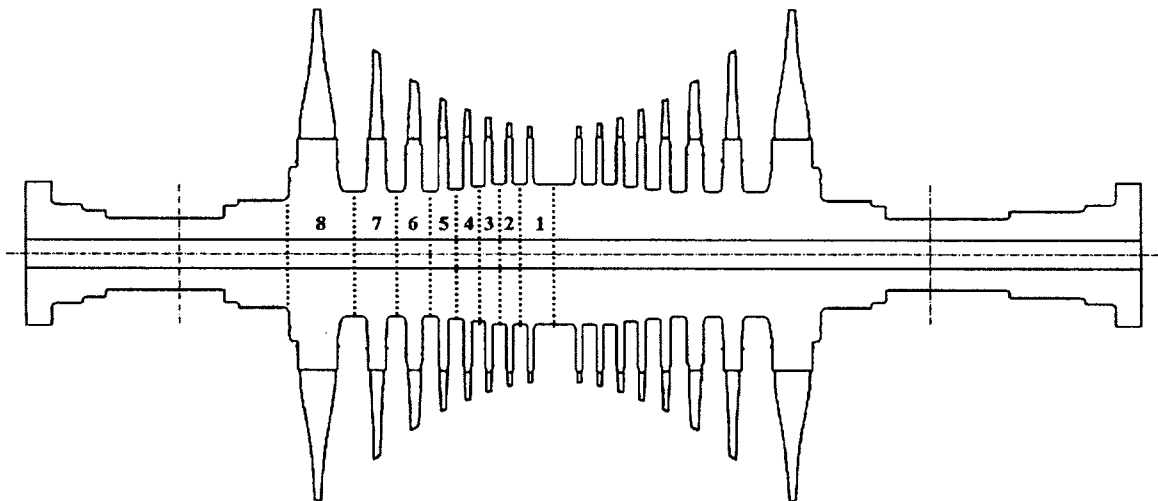
Tests have been performed by a number of investigators in which model turbine discs have been spun to failure. The results demonstrate that ductile failure can be predicted by assuming that at burst the average tangential stress is equal to the tensile strength of the disc. By knowing the stress required for failure, it is possible to calculate the speed at which failure would occur. This has been accomplished using a finite difference analysis method, [

], which calculates the average tangential stress at any given speed. For this analysis, the integral rotor body is treated as individual discs as shown in Table 4-1. To be conservative, it is assumed that failure occurs when the average tangential stress in any individual disc equals the []^{b,c} of that disc, rather than the tensile strength.

The results of this analysis are summarized in Table 4-1. From this analysis, we conclude that ductile bursting of the rotor will not occur until the speed of the rotor is increased to greater than []^{b,c} of rated speed, even when evaluated conservatively using []^{b,c}. Since this is well beyond the design overspeed, the rotor cannot fail by this mechanism unless the []^{b,c} fails to function. Therefore, the probability of this event is determined by the []^{b,c} and periodic rotor inspections have no effect on the probability of failure by this mechanism.

Table 4-1 Fully Integral Rotor Safety Factors Considering Ductile Bursting

Disc	Temp (°C)	Bore Yield Strength At Temp (MPa)	Avg. Tang. Stress at Rated Speed (MPa)	Safety Factor Bore Y.S. Avg. Tang Stress	$\frac{\text{Burst Speed}}{\text{Rated Speed}}$ $\sqrt{\frac{\text{Bore Y.S.}}{\text{Avg. Tang Stress}}}$
1					b,c
2					
3					
4					
5					
6					
7					
8					



4.2 FRACTURE RESULTING FROM HIGH CYCLE FATIGUE CRACKING

In this scenario, it is postulated that a failure can occur from a fatigue crack, which propagates in a plane transverse to the rotor axis as a result of cyclic bending loads on the rotor. These loads are developed by gravity forces and by possible misalignment of the bearings. Missile generation by this mechanism is highly unlikely since:

1. Large safety factors used in the design minimize the initiation and propagation of a fatigue crack.
2. A large transverse crack will create an eccentricity and the resulting high vibrations will cause the unit to be removed from service before fracture occurs.

However, to assure that rotor burst by this scenario will not occur during service operation, the following were evaluated:

1. Strength over stress ratios,
2. The likelihood of formation of a high-cycle fatigue crack, and
3. The propagation of a pre-existing crack by high-cycle fatigue.

Strength to stress ratios and the likelihood of initiating a high cycle fatigue crack are evaluated by comparing the magnitude of the bending stress with the failure stress, σ_{fail} , obtained from a Goodman Diagram and reduced to account for size effects. The safety factors obtained for three representative sample rotors are presented in Table 4-2. From this table, it is seen that the minimum safety factor at location []^{b,c} is more than 3.0 in all three rotors (see figure in Table 4-2 below). Therefore, from the viewpoint of crack initiation, these rotors have sufficient strength against high-cycle fatigue fracture.

The propagation of a postulated pre-existing crack is evaluated as follows:

The rotors have the threshold stress intensity range, ΔK_{th} , for fatigue crack propagation that is obtained from the relation:

$$\Delta K_{th} = F \cdot \Delta \sigma \sqrt{\pi \cdot a} \quad (4.1)$$

where $\Delta \sigma$ is the alternating bending stress, and a is the existing crack size. The flaw shape parameter F , is obtained from the equation below:

$$F = \sqrt{Q/1.21} \quad (4.2)$$

where Q , which is determined by assuming semi-elliptical crack at the material surface, and where a depth to length ratio of about []^{b,c} is applicable $Q = []^b$.

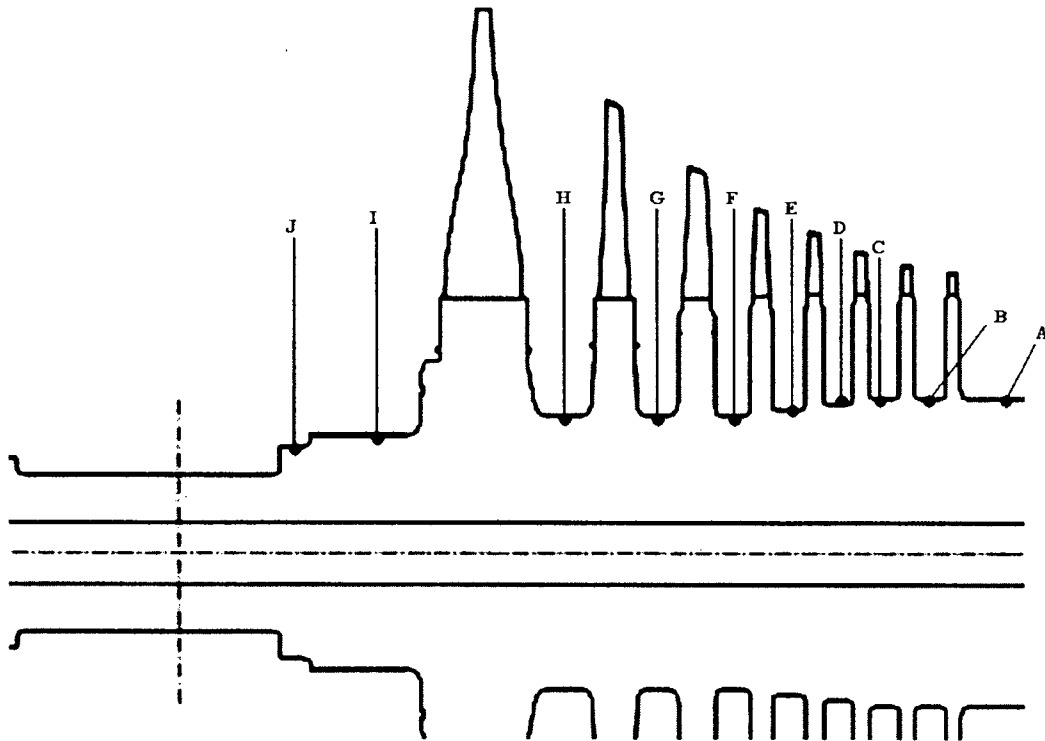
It is conservatively assumed that the threshold stress intensity range, ΔK_{th} , is $2.5 \text{ MPa}\cdot\text{m}^{1/2}$ (general alloy steel) and the minimum allowable crack size, a_{min} , is []^{b,c} mm (the assumed maximum undetectable crack size) leads to estimation of the minimum allowable vibration stress, $\Delta\sigma_{al}$, as:

$$\Delta\sigma_{al} = \Delta K_{th} \cdot \sqrt{\frac{1.21}{Q \cdot \pi \cdot a_{min}}} = []^{b,c} \quad (4.3)$$

When compared to the peak stress on Table 4-2, it can be seen that all of the peak stresses, $\Delta\sigma_{peak}$, are well below $\Delta\sigma_{al} = []^{b,c}$. This shows that the rotors have a safety margin on the propagation of a postulated pre-existing crack.

From the above analyses, it is seen that the rotors have large safety factors against high-cycle fatigue. Therefore, periodic in-service inspections for transverse fatigue fractures are not required for the AP1000 low pressure rotors.

Table 4-2 High Cycle Fatigue Peak Alternating Stresses and Safety Factors										
Location	A	B	C	D	E	F	G	H	I	J
$\Delta\sigma_{\text{fail}}$, MPa										
LP-1										
LP-2										
LP-3										
$\Delta\sigma_{\text{PEAK}}$, MPa										
LP-1										
LP-2										
LP-3										
Safety Factors										
LP-1										
LP-2										
LP-3										



4.3 FRACTURE RESULTING FROM LOW-CYCLE FATIGUE - STARTUP/ SHUTDOWN CYCLES

An analysis was carried out to determine the turbine missile generation due to a startup/shutdown cycle fatigue crack growth. In this postulated scenario, the failure mechanism is a brittle fracture, where a crack initiates in an axial-radial plane at the bore of a fully integral rotor and grows to a critical size as result of speed cycling during the operating life of the turbine.

The number of cycles to create such a failure depends on the magnitudes of and interrelationships among the following six factors:

1. The size of cracks in the bore at the beginning of turbine operation
2. The shape of these cracks
3. The size of the critical crack (dependent on the stresses experienced at running speed or design overspeed and toughness of the rotor)
4. The magnitude of the range of stress cycles experienced during the operation of machine
- 5&6. The two parameters, C_0 and n , in the Paris fatigue crack growth rate equation:

$$\frac{da}{dN} = C_0 (\Delta K)^n \quad (4.4)$$

where da/dN is the crack growth rate (per cycle), ΔK the stress intensity range, and n and C_0 are parameters of the fatigue crack growth rate equation which are determined experimentally.

The number of cycles for failure, N_f , is expressed by the following equation.

$$N_f = \frac{2}{(n-2) \cdot C_0 \cdot M^{n/2} \cdot \Delta \sigma^n} \left(a_i^{-(n-2)/2} - a_{cr}^{-(n-2)/2} \right) \quad (4.5)$$

where

- $M = 1.21\pi/Q$, Q being the flaw shape parameter
 a_i = Initial largest crack depth
 a_{cr} = Critical crack depth
 $\Delta \sigma$ = Range of stress cycles in operation.

The flaw shape parameter, Q , is determined by assuming that a semi-elliptical crack, with a depth-to-length ratio of about $[]^{b,c}$ formed at the bore surface. Such a flaw crack shape parameter would be no more than $[]^{b,c}$, independent of the stress. Therefore, Q is set to $[]^{b,c}$, conservatively.

The critical crack size, a_{cr} , is obtained from the relation:

$$a_{cr} = \frac{Q}{1.21 \cdot \pi} \left(\frac{K_{IC}}{\sigma} \right)^2 \quad (4.6)$$

where K_{IC} is the fracture toughness of the rotor and σ is the stress at operating speed and design overspeed.

The bore stress at the last stage wheel is used, and the evaluated values are []^{b,c} MPa, []^{b,c} MPa, respectively, at running speed and design overspeed of 120%. The fracture toughness, K_{IC} , is taken to be []^{b,c} MPa \sqrt{m} at the last stage wheel based on the lower limit curve for the fracture toughness of the several rotor materials. This value is much less than []^{b,c} MPa \sqrt{m} , which is estimated from the []^{b,c} correlation of Charpy V-notch energy and yield strength at upper shelf temperature.

The size of the initial crack depth, a_i , is taken to be []^{b,c} mm since the inspection procedures used for fully integral rotor forgings will reliably detect flaws as small as []^{b,c} mm deep, which is considered with the depth-to-length ratio of about []^{b,c}.

The range of $\Delta\sigma$ is taken from the expected range of stress occurring during a start-up to running speed cycle.

The values of C_0 and n in the Paris fatigue crack growth rate equation are []^{b,c} mm/cycle and []^{b,c}, respectively. These values are obtained from the upper limit curve of the normal distribution from the several materials data.

The results of the above calculation are summarized in Table 4-3. It shows that the numbers of cycles for the generation of missiles by this mechanism are extremely large. If it is assumed that the turbine operates weekly start-up/shutdown cycle, the operation life considering this failure mechanism is more than [] years. Therefore, rotor burst by this scenario will not occur.

Table 4-3 Rotor Brittle Rupture Probability Due to Startup/Shutdown Cycle Fatigue Crack Growth		
Speed Condition	Running Speed	120% Design Overspeed
Critical Crack Size, a_{cr} (mm)	[] ^{b,c}	[] ^{b,c}
Number of Cycles for Failure, N_f	[] ^{b,c}	[] ^{b,c}

4.4 FAILURE DUE TO STRESS CORROSION CRACKING

An analysis was performed to determine the probability of a fully integral rotor bursting due to stress corrosion cracking. A crack is assumed to initiate at the rim where the stresses are highest, and propagate radially inward until it reaches the critical crack size for bursting. The probability of rotor fracture due to this failure mechanism is a function of the probability of crack initiation, the rate at which a crack could grow due to stress corrosion, and the critical crack depth that will lead to a burst at either the running speed or the design overspeed. Each of these factors is discussed below.

For this analysis, it is only necessary to consider the []^{b,c} integral discs on the rotor. During operation []^{b,c} are surrounded with superheated steam. Experience has demonstrated that stress corrosion cracking does not occur in dry steam.

The probability of missile generation due to stress corrosion crack is obtained from the following equation:

$$P_{SCC} = q_i \cdot q_{cr} \cdot q_{os} \quad (4.7)$$

where,

q_i is the probability of crack initiation

q_{cr} is the probability of flaw propagation until critical crack size on stress corrosion crack mode

q_{os} is the probability that the unit will reach design overspeed

For conservative evaluation of this probability, it is assumed that q_i , which is the probability of crack initiation, is 100%, even though we have not experienced finding cracks on fully integral nuclear low pressure rotors at inspection through 2006. Also, q_{os} is assumed to be 100%, even though it is actually on the order of 10^{-5} , with proper maintenance of the turbine valve and control system. Therefore, the probability of missile generation due to stress corrosion crack is obtained conservatively by this analysis.

Furthermore, we have not experienced stress corrosion cracking on fully integral nuclear low pressure rotors, which are designed with relatively low yield stress materials, $\sigma_{ys} \approx []^{b,c}$ MPa, compared to center shaft built-up rotors, which have keyways. However, this probability analysis due to stress corrosion cracking is based on experimental high yield stress materials data, because it has the same composition, 3 1/2% Ni-Cr-Mo-V rotor steel.

4.4.1 Probability of Crack Initiation

The probability of crack initiation in disc i , q_i , is obtained from inspection records of nuclear turbines with built-up rotors, and is calculated for each disc number within each turbine style. This gives conservative estimates since the built-up rotors have stresses and yield strengths, which are significantly higher than those of fully integral rotors.

Suppose that N number i discs in a particular turbine style have been inspected and a total of K have been found with one or more cracks. We take:

$$[\quad]^{b,c} \quad (4.8)$$

for any number i disc in that particular turbine style.

We have not experienced finding any cracks during the inspection of 22 existing rotors. However, for conservative estimation, the probability of crack initiation is assumed to be 100%.

4.4.2 Crack Growth Rates

The crack growth rate model used is as follows:

$$[\quad]^{b,c} \quad (4.9)$$

where,

$$[\quad]^{b,c}$$

The actual values used for the parameters on the crack growth rate model are the same as those used for keyway stress corrosion crack growth rate in built-up rotors. These values are:

$$\begin{aligned} & [\quad]^{b,c} \\ & [\quad]^{b,c} \\ & [\quad]^{b,c} \end{aligned}$$

For $[\quad]^{b,c}$, a normal distribution with a mean value of $[\quad]^{b,c}$ calculation is used. The distribution of $[\quad]^{b,c}$ is obtained from fatigue crack growth rate data presented in Table 4-4. The data includes different materials from the AP1000 rotor, and can be regarded as having the larger deviation of term uncertainty than the data of the AP1000 rotor material, 3 1/2% Ni-Cr-Mo-V. Using the larger deviation, the higher probability is calculated, therefore, the calculation results become more conservative.

The calculations were carried out for the $[\quad]^{b,c}$ of eight low pressure turbine discs using the maximum numerical average temperatures at the inlet faces of each disc.

Table 4-4
3 1/2% Ni-Cr-Mo-V Rotor Steel Deviation Crack Growth Rate from Calculation

Data Source	Growth Rate from Calculation *10 ⁻⁴ mm/h	Growth Rate from Experiment *10 ⁻⁴ mm/h	Logarithm Deviation
1	1.2	1.3	-0.114
2	1.2	0.2	1.555
3	1.2	2.3	-0.645
4	1.5	1.5	-0.035
5	1.5	2.3	-0.427
6	1.6	2.0	-0.209
7	1.6	2.7	-0.544
8	1.7	2.6	-0.400
9	1.7	3.0	-0.539
10	1.7	4.1	-0.849
11	2.8	3.2	-0.131
12	2.8	3.5	-0.207
13	2.8	3.1	-0.074
14	3.2	4.9	-0.431
15	3.2	2.7	0.163
16	3.2	3.0	0.043
17	3.2	3.3	-0.033
18	3.2	3.5	-0.096
19	3.2	1.4	0.782
20	2.0	2.5	-0.217
21	2.0	1.7	0.155
22	2.0	2.3	-0.123
23	2.0	3.2	-0.470
24	2.0	3.8	-0.635
25	2.0	4.2	-0.736
26	5.3	6.8	-0.252
27	5.3	9.8	-0.619
28	5.3	8.3	-0.455
29	5.3	8.8	-0.511

Table 4-4
3 1/2% Ni-Cr-Mo-V Rotor Steel Deviation Crack Growth Rate from Calculation

Data Source	Growth Rate from Calculation *10 ⁻⁴ mm/h	Growth Rate from Experiment *10 ⁻⁴ mm/h	Logarithm Deviation
30	1.1	0.6	0.635
31	1.1	1.1	0.022
32	1.1	1.5	-0.275
33	1.6	0.5	1.086
34	1.6	0.8	0.694
35	1.6	0.8	0.618
36	1.6	1.0	0.486
37	1.6	1.0	0.416
38	1.6	1.2	0.296
39	1.6	1.5	0.068
40	1.6	1.9	-0.210
41	5.3	8.1	-0.421
42	5.3	8.8	-0.497
43	5.3	6.2	-0.156
44	5.3	7.0	-0.276

4.4.3 Critical Crack Size

The critical crack depths were obtained for []^{b,c} of fully integral rotors, with []^{b,c} MPa yield strength, by using the relationship between fracture toughness and stress intensity. Stress intensity factors were determined at running speed and 120% overspeed. In each case, the influence of thermal stress was included. The thermal stress used was that determined to be the most severe during a transient condition. At running speed, the stress intensity for all crack depths less than the total depth of the disc was well below the fracture toughness. Therefore, it is conservatively assumed that the total depth of the disc is the critical crack depth on running speed. A limit load analysis confirms that ductile fracture of the rotor would not occur under these conditions.

The depth of the disc is taken as the distance between the rim of the disc and the point where it blends into the main body of the rotor.

In determining critical crack size at overspeed, we use the relationship between fracture toughness and stress intensity. The relationship is obtained as follows:

$$K_{IC_SCC} \geq K_I = \phi \cdot \sigma \sqrt{\pi \cdot a} \quad (4.10)$$

If the above equation can be satisfied, rotor burst will occur by stress corrosion crack growth. Thus, for conservatism, a larger stress, $\sigma' \equiv n \cdot \sigma$, stress at overspeed is utilized as is a smaller critical crack size, a' . Rotor burst is as follows:

$$a' = \frac{K_I^2}{\phi^2 \cdot \pi} \cdot \frac{1}{\sigma'^2} \equiv \frac{1}{n^2} \cdot a \quad (4.11)$$

The critical size at 120% overspeed is:

$$a_{cr_os} = \frac{1}{1.4^2} \cdot a_{cr} \quad (4.12)$$

4.4.4 Numerical Results

With the distributions of crack growth rates and critical crack sizes described in the previous sections, analyses were made to determine the probability that a crack would grow to the critical size within any time interval, t . To get the probability of a rotor bursting, this probability is modified by the number of discs being considered, the probability of crack initiation, and for the design overspeed conditions, the probability that the unit will reach design overspeed.

Since, the probability that the unit will reach design overspeed has been unknown, its probability is assumed to be 100% to evaluate the probability of missile generation conservatively.

The final probability values are given in terms of discrete inspection intervals in Table 4.5 and are shown graphically in Figure 4-1. The results show that the inspection interval needed to satisfy the requirement that the probability of missile generation be less than 1.0E-05 per year is over []^{b,c} years, given the conservative assumptions incorporated by this analysis.

Table 4-5 Probability of Rotor Rupture Due to Stress Corrosion			
Probability of Rotor Rupture at			
Inspection Interval(yrs)	Running Speed		120% Design Overspeed
12.0			b,c
16.0			
20.0			
24.0			
28.0			
32.0			
36.0			
40.0			

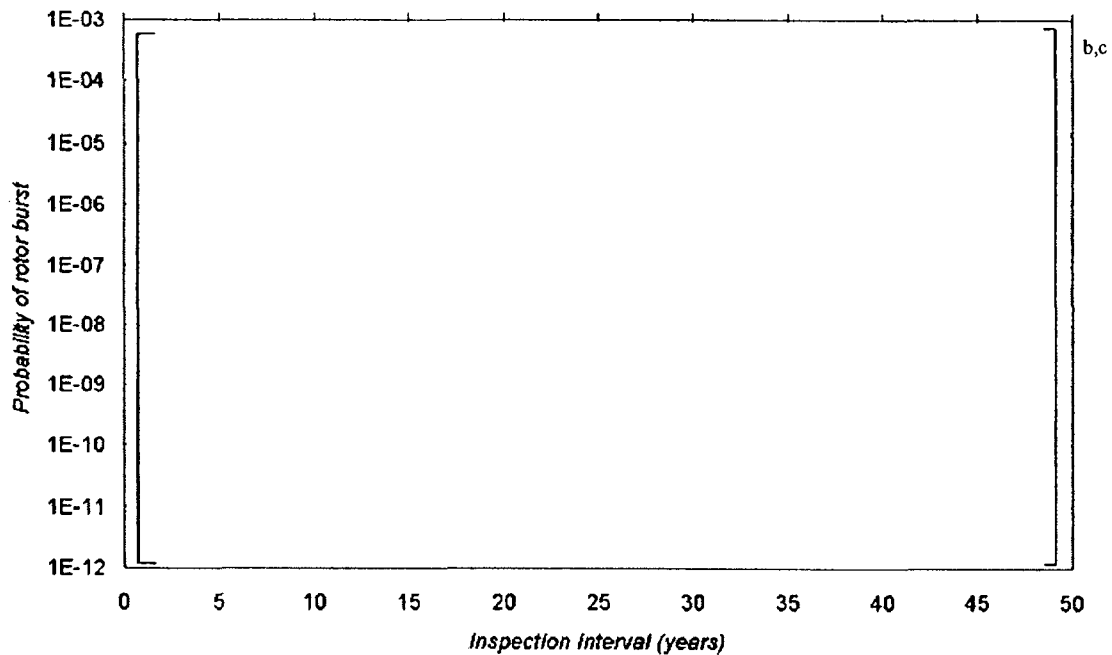


Figure 4-1 Probability of Rotor Rupture Due to Stress Corrosion

5. DISCUSSION AND CONCLUSIONS

Except for the destructive overspeed mechanism, this report demonstrates that the fully integral AP1000 low pressure rotor design is unlikely to generate a missile by any of the mechanisms considered. The probability of reaching destructive overspeed is primarily dependent upon []^{b,c}. Reference 11 addresses that issue.

The low pressure rotors are not likely to burst as a result of a high-cycle fatigue mechanism since the maximum alternating stress is less than the endurance stress obtained from the Goodman diagram, and their safety factors are greater than 3.0. Additional assurances against bursting by this mechanism are derived from the following:

1. In fully integral rotors, the locations of maximum stress are readily accessible for inspection during normal maintenance.
2. Bursting by this mechanism is unlikely, since the existence of a large transverse crack is detectable by high vibrations due to rotor unbalance.

It is reasonable to eliminate high cycle fatigue as the controlling mechanism for determining in-service inspection intervals.

Analysis of the low cycle fatigue mechanism demonstrates that the number of cycles for failure by this scenario is extremely large, even when utilizing highly conservative assumptions. Periodic in-service inspections for low cycle fatigue cracks will not contribute significantly to improvement in safety. Therefore, low cycle fatigue is also eliminated as the controlling mechanism for determining inspection intervals.

As with previous designs, the potential for stress corrosion cracking has the greatest influence on rotor integrity. However, in fully integral designs, such as that used in the AP1000 low pressure rotors, the probability of failure by this mechanism has been reduced. The analysis shows that over []^{b,c} years of running time, utilizing highly conservative assumptions, may elapse before performing safety related inspections without exceeding the NRC safety criteria. Considering typical use factors for nuclear turbines, and considering that the crack locations are readily observable during normal turbine maintenance, it is concluded that periodic safety related inspections are not required within the expected life of the turbine.

6. REFERENCES

1. Sawada, S., Tokuda, A., Homma, R. and Jin, T., "Manufacture of the Low Pressure Turbine Rotor Forgings with High Strength and Good Toughness," JSW Technical Review, No.12, pp.11-20, 1976.
2. Barson, J.M. and Rolfe, S.T., "Correlations Between KIC and Charpy V-Notch Test Results in the Transition Temperature Range," Impact Testing of Metals, ASTM STP 466, 1970, pp. 281-302.
3. Walden, N.E.; Percy, M.J.; and Mellor, P.B., "Burst Strength of Rotating Discs," Proceedings of the Institute of Mechanical Engineers, 1965-66.
4. Greenberg, H.D. et al, "Critical Flaw Size for Brittle Fracture of Large Turbine Generator Forgings," 5th International Forgemaster Meeting (Temi), 1970.
5. Robinson, E.L., "Bursting Tests of Steam Turbine Disc Wheels," ASME Annual Meeting, 1943.
6. Paris, P.C., "The Fracture Mechanism Approach to Fatigue," Fatigue –An Interdisciplinary Approach, Proc. 10th Sagamore Army Materials Research Conference, Syracuse University Press, 1964.
7. Inagaki, S., Miyazaki, M., Kashiwaya, H. and Nakadai, K., "Effects of Material and Environmental Factors on SCC of NiCrMoV Rotor Steels," EPRI Fossil Steam Turbine Disc Cracking Workshop, 1990.
8. Lyle Jr., F.F. and Burghard Jr., H.C., "Steam Turbine Disc Cracking Experience," EPRI NP-2429-LD RP 1389-5, Vol.1-7, 1982.
9. Roberts, B.W. and Greenfield, P., "Stress Corrosion of Steam Turbine Disc and Rotor Steels," CORROSION-NACE Vol. 35, No.9, p.402, 1979.
10. Clark Jr., W.G., Seth, B.B. and Shaffer, D.H., "Procedure for Estimating the Probability of Steam Turbine Disc Rupture from Stress Corrosion Cracking," the Joint ASME/IEEE Power Generation Conference, 81-JPGC-Pwr-31, 1981.
11. []^{b,c}